ACS Sustainable Chemistry & Engineering

Research Article

pubs.acs.org/journal/ascecg

Beyond a Model of Polymer Processing-Triggered Shear: Reconciling Shish-Kebab Formation and Control of Chain Degradation in Sheared Poly(L-lactic acid)

Huan Xu,[†,‡] Lan Xie,*[,‡,§] and Minna Hakkarainen*[,†]

[†]Department of Fibre and Polymer Technology, KTH Royal Institute of Technology, Stockholm 100 44, Sweden

[‡]College of Polymer Science and Engineering, State Key Laboratory of Polymer Materials Engineering, Sichuan University, Chengdu 610065, China

[§]Department of Materials Science and Engineering, University of Sheffield, Sheffield S1 3JD, United Kingdom

Supporting Information

ABSTRACT: Here we disclose an unprecedented methodology toward high-performance poly(L-lactic acid) (PLLA) through generation of dense shish-kebabs, while the normal shear stress-induced chain degradation is controlled. The key elements involve the application of a pulse of strong shear and controlled crystallization. Specifically, the shear featuring a short duration of 1 s and a shear rate high to 100 s^{-1} was employed to create shish precursors, which was followed by high-temperature crystallization (at 130, 135, and 140 °C) to render the prevailing development of shish-kebabs rather than spherulites. The direct observation of the overgrown shish afforded the demonstration of its origin from shear-aligned bundles of fibrillar chains, implying the crucial importance of chain entanglements in driving the alignment of neighboring chains along the transient shear. For the first time, the shear-aligned shish was revealed to present much higher conformational order, compared to the neighboring kebabs or spherulites. It is of great interest that the application of transient shear flow prevented PLLA from shear-induced degradation, although the PLLA chains are inherently sensitive to external shear stress. The proposed pathway, thus, creates PLLA rich in shish-kebabs with well-preserved high-molecular-weight chains. This signifies a new scenario with respect to previous studies where strong and long-acting shear was required for the formation of oriented structures in PLLA and the property enhancement was to large part hampered by simultaneous chain scissions. Of immense significance is the possibility to utilize these findings during common processing such as extrusion, spinning, and blowing, in which a transient and intensive shear flow is normally generated.

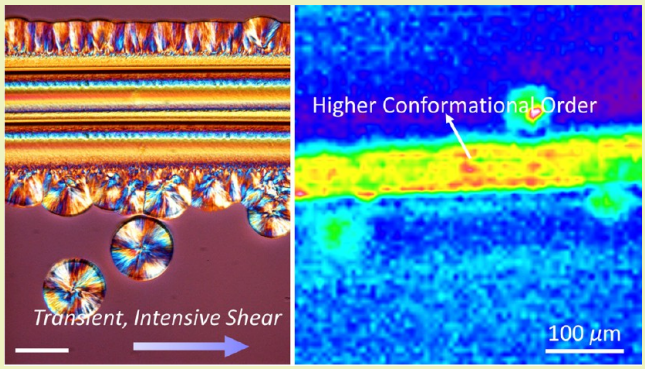

KEYWORDS: *A pulse of shear, Poly(L-lactic acid), Cylindrite, Shish-kebab, Conformational ordering, Chain degradation*

INTRODUCTION

Through the long river of investigations on controlling the crystallization behaviors of semicrystalline polymers, the unique shish-kebab superstructure, consisting of symmetrical ordered kebabs strung by a central oriented shish, never fails to catch the interest of both the academic researchers and the technical community.[1−4] This is further pushed forward with the advent of cutting-edge detection techniques, such as neutron scattering combined with atom labeling,[5] synchrotron X-ray measurements with high spatial resolution and high time resolution,[6−8] and high-speed optical microscopy observations.[9] Serving as an excellent self-reinforcing element, the controllable generation of shish-kebab structures during polymer processing has demonstrated significant benefits to the mechanical properties (e.g., strength and stiffness) of both polyolefins and polyesters.[10−13] It is pertinent to point out that, although much effort has been devoted to developing shish-kebab structures in traditional plastics such as polyethylene and polypropylene,[14−16] it still remains a great challenge to establish oriented crystalline superstructures in biodegradable polymers. This strategy, though, represents enormous potential for facilitating the industrial revolution of the emerging bioplastics market.[17−20] Central to this challenge is the undesirable chain characters embodied in biopolymers and bioplastics, basically featuring low steric regularity, rigid molecular backbones and/or low molecular weight.[6,21] It appears that, when targeting shish-kebab formation, normally a strong (high shear rate), long-acting (large shear strain) shear is supposed to be a prerequisite to adequately stretch and orient biopolymer chains, and to suppress the relaxation or disengagement of oriented seg-

Received: March 3, 2015
Revised: May 21, 2015
Published: May 25, 2015

DOI: 10.1021/acssuschemeng.5b00320
ACS Sustainable Chem. Eng. 2015, 3, 1443−1452

ments.[22] This lays down special technical bottlenecks, as an example, in an endeavor to form rich shish-kebabs in injection-molded poly(L-lactic acid) (PLLA) we utilized a fierce and continuous shear flow with a shear rate of ~220 s^{-1} for nearly 3 min.[18]

Long exposure to strong shear and high temperature, however, creates the huge risk in altering the molecular weight and molecular weight distribution due to the mechanical and thermal degradation, especially in the case of biopolyesters.[23] This is exemplified by the distinct decrease in weight-average molecular weight (M_w) and rise in polydispersity observed for PLLA during extrusion followed by compression molding.[24] It also explains the limited enhancement of tensile strength to 73.7 MPa for sheared PLLA from the initial value of 64.9 MPa for the control sample.[18] This is in sharp contrast with the nearly doubled tensile strength in the case of linear low density polyethylene containing shish-kebabs.[25] Apparently, the performance improvements from the contributions of PLLA shish-kebabs are dwarfed by the scissions of long chains, which are to large extent responsible for the stress transfer and impact resistance.[26] More importantly, such a time and energy-consuming shear processing aimed at manufacturing shish-kebab-rich polymeric materials may largely push up the production costs, imposing distinct disadvantages for exploiting biopolymers and bioplastics as competitive candidates for substituting the petroleum-based traditional plastics.[27]

This dilemma inspires us to attempt the launch of shish-kebab formation in bioplastics in an energetically favorable manner, to explore the possibility to establish numerous shish-kebabs by virtue of a transient shear flow (a shear time low to 1 s), an extremely short-lived shear action that is rarely employed. PLLA, an increasingly popular biobased polymer, was chosen as the model polymer, appraised from the following viewpoints: on one side, PLLA is well renowned as the most promising green polymer due to its satisfactory biocompatibility, desirable renewability and degradability;[28−31] on the other hand, there exists an urgent scientific imperative requiring the optimization of the mechanical and thermal performances of PLLA to remove the application constraints in structural materials, beverage and food packaging and biomedical fields. Tailoring the performances through crystalline morphology control provides a straightforward methodology.[32−36] In general, a pulse of incredibly intensive shear flow is involved during the common processing of PLLA, such as melt and electrospinning, blowing, injection molding and extrusion. Surprisingly, the possibility to develop shish-kebab-rich PLLA during the transient shear has not been examined. Herein, we attempt to map the structural evolution of PLLA in the transient shear flow, particularly the origin of shish, which may open new opportunities to manipulate the oriented superstructures during common processing and aid the material scientists to design processing principles for achieving high-performance bioplastic products.

EXPERIMENTAL SECTION

Materials and Sample Preparation. A widely used commercial PLLA resin under the trade name of 4032D, comprising around 2% D-LA, was kindly provided by NatureWorks (USA). To obtain thin PLLA films with a specific thickness of ~20 μm, dried PLLA was dissolved in chloroform (VWR, Germany) and then carefully dripped onto a glass slide followed by absolute volatilization of solvent under vacuum at 80 °C. The as-prepared PLLA films were melted on a Linkam CSS450 shear stage at 200 °C for 5 min, then the upper lid gently fell down to compress homogeneously the melted films, finally ending at the gap of 10 μm. Note that such a low gap enabled the compact contact between the lids and PLLA melts. A transient but strong shear flow, featuring a short duration of 1 s and a high shear rate of 100 s^{-1} was applied onto the PLLA melts once the melts were cooled down to the crystallization temperatures, i.e., 130, 135, and 140 °C. The shear duration of 1s was the limit we can apply using the shear system. The sheared melts were isothermally crystallized for 60 min, while static control samples without application of shear action were submitted to the same temperature protocol. Figure 1 schematically depicts the temperature and shear protocol. After isothermal crystallization, the static and sheared samples were carefully taken out for morphological observation and structural determination.

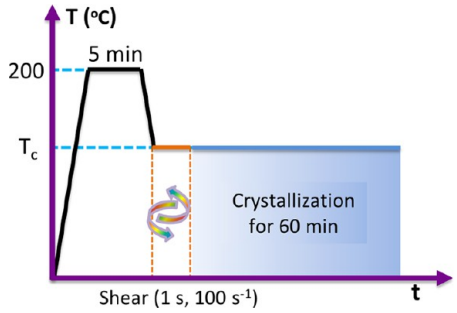

Figure 1. Temperature and shear protocol applied to conduct static and shear-induced crystallization of PLLA. A transient (duration of 1 s) but strong (shear rate of 100 s^{-1}) shear flow was applied immediately once the PLLA melts were cooled to the preset crystallization temperature (T_c), whereas the control samples were isothermally crystallized without shear application.

Polarized Optical Microscopy (POM) and Scanning Electron Microscopy (SEM) Observations. An Optiphot 2 microscope equipped with a Leica digital camera was applied to observe the crystalline morphology developed in the static and sheared PLLA. For SEM observation, the sheared and crystallized films were etched in a water−methanol (1:2, v:v) solution containing 0.025 mol/L of sodium hydroxide and 1 mol/L of sodium chloride for 16 h at 10 °C. An SE-4800 SEM (Hitachi, Japan), operating at a low accelerated voltage of 0.5 keV to avoid demaging matrix, was utilized to characterize shear-induced crystalline morphology. Prior to SEM observation, all samples were sputter-coated with a 3.5 nm-thick gold layer.

Two-Dimensional Wide-Angle X-ray Diffraction (2D-WAXD) and Two-Dimensional Small-Angle X-ray Scattering (2D-SAXS) Measurements. To identify the structural features for the oriented crystalline entities developed in the sheared PLLA samples, 2D-WAXD and 2D-SAXS measurements were carried out using a homemade laboratory instrument (Bruker NanoStar, Cu Kα radiation) in the Crystallography Lab, Department of Molecular Biology and Biotechnology, University of Sheffield. The X-ray beam with a wavelength of 0.157 nm was focused to a tiny area of 4 × 4 μm, and the distance from sample to detector was held at 350 mm and 1850 mm for WAXD and SAXS measurements, respectively. An X-ray CCD detector (Model Mar345, a resolution of 2300 × 2300 pixels, Rayonix Co. Ltd., USA) was employed to collect the 2D images. Crystallinity and molecular orientation degree (f_H) were quantitatively analyzed based on 2D-WAXD data. Specifically, the WAXD intensity profiles for each 2θ were obtained by integration in the azimuthal angular range of a whole circle (0−360°) from the diffraction patterns. The intensity profiles were further processed using the Origin 7.5 software, assuming Gaussian profiles for the amorphous halo and all crystalline peaks, and the crystallinity was determined by the ratio of the area under the resolved Gaussian crystalline peaks to the total area under the unresolved diffraction curve. To evaluate the molecular orientation of PLLA, f_H was calculated mathematically using Picken's method based on the azimuthal angle of lattice plane (200)/(110). Lamellar structures in the sheared PLLA were examined by virtue of SAXS, the radically integrated intensities $I(q)$ ($q = 4\pi\sin\theta/\lambda$) were obtained for

DOI: 10.1021/acssuschemeng.5b00320
ACS Sustainable Chem. Eng. 2015, 3, 1443−1452

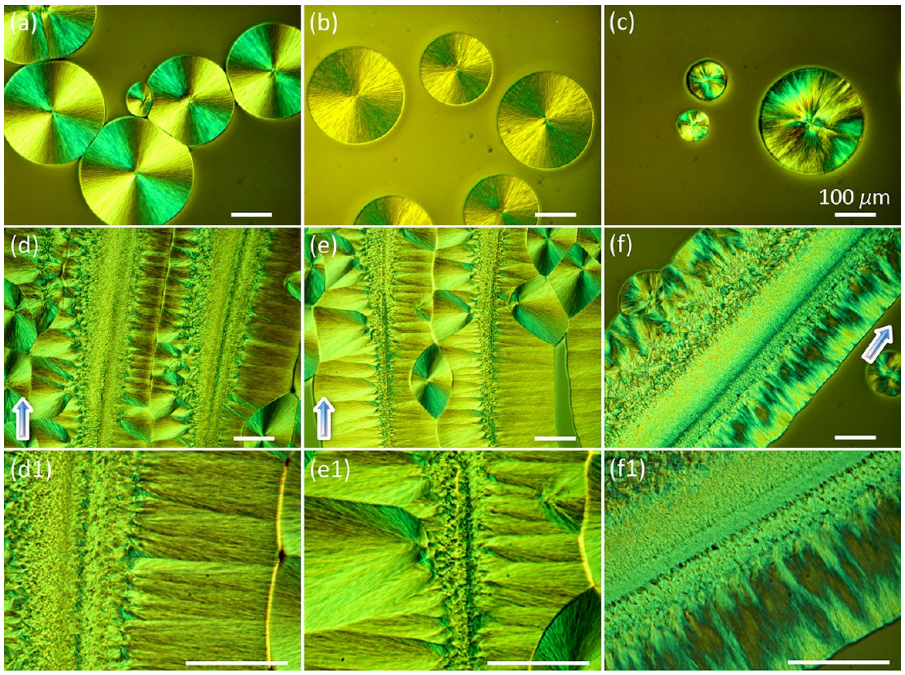

Figure 2. POM micrographs showing the crystalline morphology developed in the (a−c) static and (d−f) sheared PLLA melts after isothermal crystallization for 60 min at (a, d) 130, (b, e) 135, and (c, f) 140 °C. Panels d1−f1 present the local observation for panels d−f, respectively. The arrows indicate the flow direction, and the scale bars represent 100 μm.

integration in the azimuthal angular range of a whole circle, where 2θ was the scattering angle and λ represented the X-ray wavelength. The long period regarding the lamellar structure was acquired using the Bragg equation, $L = 2\pi/q^*$, where L indicated the long period, and q^* stood for the peak position in the scattering curves.

Size Exclusion Chromatography (SEC) Determination. The possible changes in macromolecular characters were examined by SEC. PLLA films were melted at 200 °C for 5 min followed by quenching to 135 °C, then a steady shear with a shear rate of 100 s^{-1} was applied on the melts for a series of shear durations, i.e., 0, 1, 30, 60, 120, 180, and 300 s. SEC determination was performed on a Verotech PL-GPC 50 Plus system equipped with a PL-RI Detector and two PolarGel-M Organic (300 × 7.5 mm) columns from Varian. The chloroform solutions containing sheared PLLA samples were injected with a PL-AS RT autosampler, and chloroform was used as the mobile phase (1 mL/min, 35 °C).

Fourier Transform Infrared Spectroscopy (FTIR) Imaging. 2D FTIR absorbance patterns were imaged using a PerkinElmer Spotlight 400 system equipped with an optical microscope (Bucks, UK). The sheared PLLA films after crystallization were directly used, while the sample thickness in the detection area was fixed at ∼10 μm to permit the direct comparison of absorbance intensity.

RESULTS AND DISCUSSION

Recently, there is growing interest in achieving mechanical property promotion by constructing oriented crystalline superstructures in biopolymers and bioplastics. Since the early 1960s, formation mechanisms for shear-induced shish-kebabs have been widely illustrated in an assortment of polyolefins, which has yielded seemingly controversial suppositions on the critical parameters of the shear flow targeted for shish-kebab formation.[37−41] Three distinguished hypotheses have been proposed to describe the critical flow parameters for shish formation, i.e., critical shear rate larger than the Rouse time to sufficiently stretch chains,[42] critical strain to fully extend chain segments,[43] and critical specific work of flow that integrates the multiple factors of time, flow geometry, and molecular weight distribution.[44,45] The fundamental understanding has been totally based on the polyolefin models.[46−48] As an example, in 2005, a pioneering exploration launched by Han's group suggested that a weak shear action (shear rate low to 0.5 s^{-1}) allowed the formation of compact cylindrical shish-kebab structures for isotactic polypropylene.[49,50] Their ongoing efforts in 2009 revealed similar observations in weakly sheared blends of isotactic polypropylene and high density polyethylene.[51] Compared to the prominent attempts on the development of aligned row nuclei for polyolefins, few scenarios of oriented supramolecular structures for biopolymers have been unfolded. The progressive findings on polyolefins contrast with the recent observations of threadlike cylindrites in continuously sheared PLLA melts during nonisothermal[52] and isothermal crystallization.[53] It appeared that a relatively long submission to strong shear flow is required to create row nuclei of PLLA. This can be exemplified by the observations of PLLA cylindrites by applying a steady shear flow of 40 s^{-1} for 5 s during the isothermal crystallization[54] and 30 s^{-1} for 180 s during the nonisothermal crystallization.[22] Could we then expect the morphological transition by an application of a pulse of shear flow for only 1 s?

Figure 2 offers a direct observation of the shear-induced crystalline morphologies. The quiescent crystallization as a control counterpart was performed prior to tracking shear-induced crystallization, and only regular spherulites were developed (Figure 2a−c), showing gradually decreased nucleation density and spherulite size with the increase of crystallization temperature. It is of great interest to observe the evident transition to highly oriented cylindrites in the sheared PLLA samples (Figure 2d−f), independent of crystallization temperature. These cylindrites featuring linear edges must be elicited through the symmetrical growth of lamellae strung by the central row nuclei. An inspection of Figure 2d1−f1 manifests that an incredibly high density of central cores orderly align along the shear flow and engage in the compact

DOI: 10.1021/acssuschemeng.5b00320
ACS Sustainable Chem. Eng. 2015, 3, 1443−1452

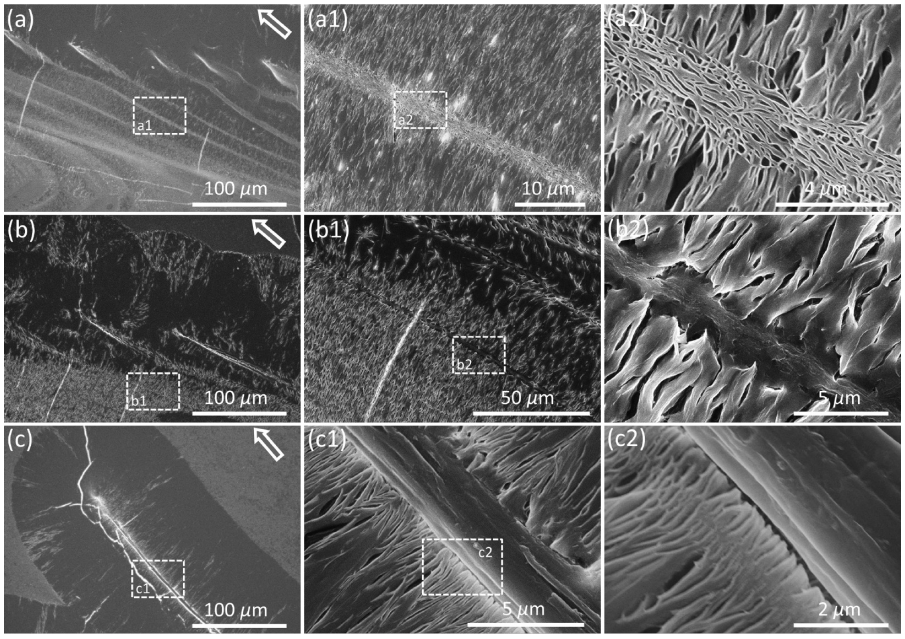

Figure 3. SEM micrographs showing the structure of cylindrites formed in the sheared PLLA melts after isothermal crystallization for 60 min at (a) 130, (b) 135, and (c) 140 °C. Panels a1−c1 and a2−c2 illustrate the local observation in the dotted rectangles of panels a−c and a1−c1, respectively. The arrows indicate the flow direction.

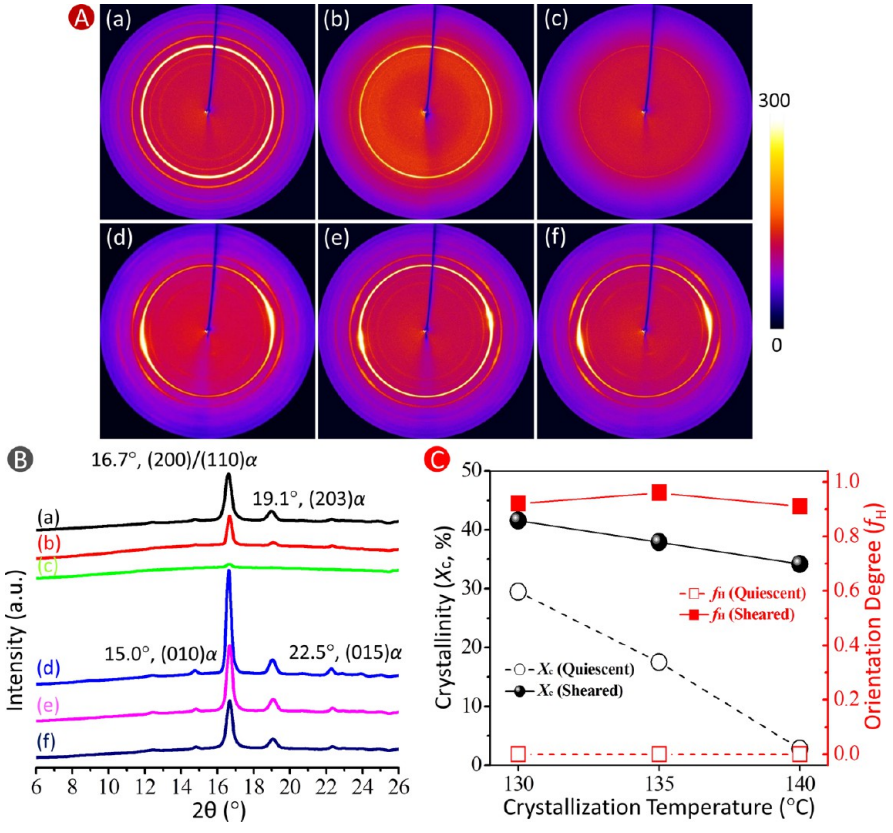

Figure 4. (A) 2D-WAXD images showing the homogeneous crystalline morphology developed in (a−c) static PLLA and highly oriented crystalline superstructures formed in (d−f) sheared PLLA during the isothermal crystallization for 60 min at (a, d) 130, (b, e) 135, and (c, f) 140 °C. (B) 1D-WAXD intensity curves extracted from panel A, the peak position and lattice plane attribution are marked on the diffraction peaks. (C) Crystallinity (X_c) and orientation degree (f_H) for static and sheared PLLA as a function of crystallization temperature.

nucleation of adjacent chains. It is worth stressing that the shear-driven high nucleation activity renders the generation of large-sized cylindrites (an average radius of around 150 μm showing weak relation to crystallization temperature), while the average radius of spherulites dramatically decreases from 115 μm (130 °C) to 62 μm (140 °C) for static PLLA. Obviously,

DOI: 10.1021/acssuschemeng.5b00320
ACS Sustainable Chem. Eng. 2015, 3, 1443−1452

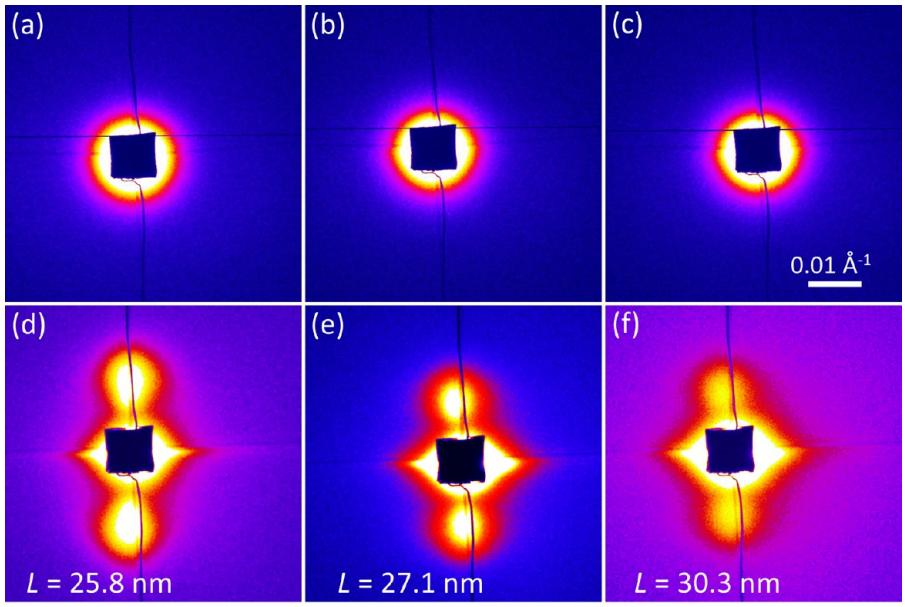

Figure 5. 2D-SAXS images demonstrating the existence of homogeneous crystalline entities in (a–c) static PLLA and the formation of classic shish-kebab superstructure in (d–f) sheared PLLA after isothermal crystallization at (a, d) 130, (b, e) 135, and (c, f) 140 °C.

utilization of shear flow presents an overwhelming superiority in tailoring the crystallization behavior of PLLA compared to the normal regulation by crystallization temperature.

Figure 3 provides high-resolution SEM examination regarding the fine structure of shear-induced cylindrites, especially for the primary row nuclei. Dense threadlike row nuclei along the flow are immediately identified in PLLA sheared and annealed at 130 °C, as shown in Figure 3a, reaching an astounding length up to several millimeters (observed during SEM operation). Figure 3a1 illustrates the symmetrical development of incredibly dense and ordered lamellae (kebabs) wrapping the central cores (shish). The kebabs aligned perpendicularly to the shish are closely connected to row nuclei. Figure 3a2 reveals some unexpected freatures for the shish structure: a straight arrangement of row nuclei, which has a diameter of 2.7 μm, linking adjacent kebabs, is clearly presented. It appears that compact fibrillar chain bundles orderly assemble into the shish, in close resemblance to the shear-driven assembly of fibrillar extended chain crystals unveiled in the sheared PLLA by gently pulling the fiber which shares the strong shear rate and short duration.[6] Figure 3b,c again confirms the hierarchical structure of cylindrites in the samples sheared at 135 and 140 °C, consisting of threadlike shish that elicits the compact alignment of kebabs in both sides. Furthermore, the shish structure is essentially associated with the organization of fibrillar extended chain bundles, unaltered by the crystallization temperature. In the continuously sheared PLLA melts (a steady shear rate of 5 s^{-1} at 150 °C), Yamazaki et al. also found macroscopic single strand with a width of 2 μm comprising a bundle of several microsized fibrils, conceiving the perspective that the observed shish structure was essentially identical with overgrown shish of polyolefins such as polypropylene and polyethylene.[53] This hypothesis is strongly supported by our observation, which in turn states that the shish superstructure likely stems from fibrillar extended chain crystals.

Two-dimensional X-ray diffraction/scattering is a workhorse of shish-kebab characterization in view of its ability to image molecular arrangement and crystal packing from microscale to nanoscale, and to provide quantitative evaluation.[55−57] Figure 4A manifests some remarkable results by comparing the 2D-WAXD patterns of static and sheared PLLA. In particular, strong diffraction arcs representing high orientation degree and crystallinity are exhibited in all sheared PLLA samples, independent of crystallization temperature, while homogeneous diffraction rings are observed for static samples whose intensity shows a constant decay with the increasing temperature. Figure 4B gathers the 1D diffraction intensity profiles extracted from the 2D diffraction patterns. Direct comparison shows that the diffraction peaks of static and sheared PLLA coincide in all the curves, which is a demonstration of the same crystal form. Furthermore, we point out that the intensity curves mainly show four distinct diffraction peaks located at 2θ = 15.0, 16.7, 19.1, and 22.5°, which are assigned to lattice planes (010), (200)/(110), (203), and (015) of α-form crystals of PLLA, respectively.[33,58] It is apparent that the application of shear flow largely enhances the crystallinity and orientation degree, as quantitatively evidenced by Figure 4C. Figure 4C reveals that high crystallinity, fluctuating between 41.6% (130 °C) and 34.2% (140 °C), is achieved for sheared PLLA samples, in contrast to the uncontrollable crystallinity of static PLLA, which declines drastically from 29.5% to 2.8% when crystallization temperature is increased from 130 to 140 °C. In particular, extremely high orientation parameters (f_H) around 0.92 are presented for all the sheared samples, profoundly revealing that the creation of oriented crystalline entities is prominently governed by shear flow rather than by crystallization temperature. It principally lies in the limited disengagement and relaxation of shear-induced oriented units at such a temperature range, rendering the long-term survival of stable primary row nuclei during the crystallization. This observation permits the assumption that the POM and SEM images indeed illustrate the successive growth of shish structures during crystallization (Figures 2 and 3), starting from primary row nuclei without thermally induced structural changes or damages.

Next, we characterized the large differences in SAXS patterns for static and sheared PLLA, as illustrated in Figure 5. The

DOI: 10.1021/acssuschemeng.5b00320
ACS Sustainable Chem. Eng. 2015, 3, 1443−1452

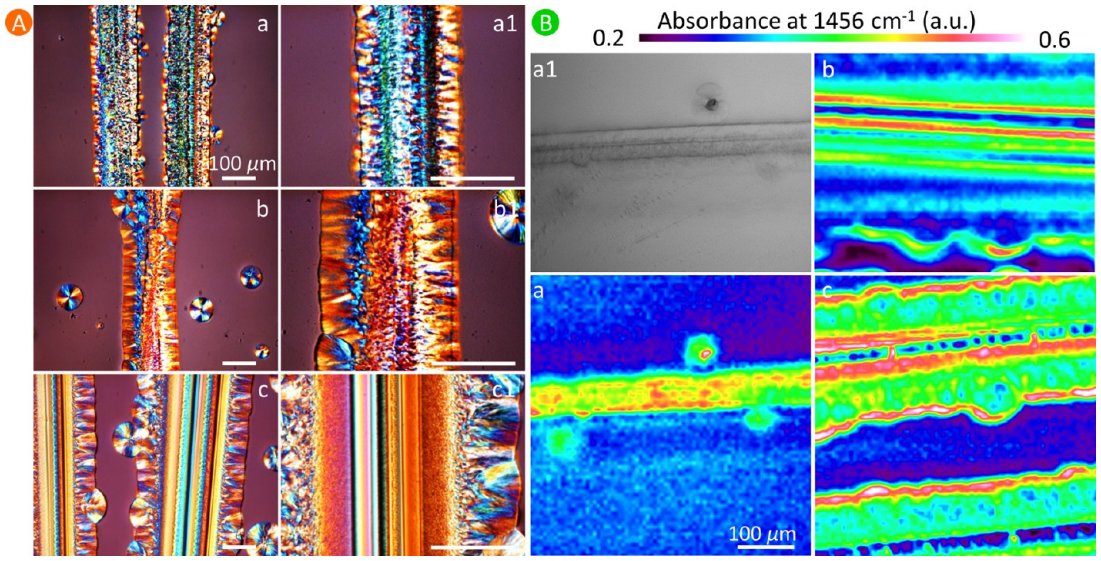

Figure 6. Structural evolution of shear-induced PLLA cylindrites during the isothermal crystallization. (A) POM images of PLLA cylindrites, panels a1−c1 show the local morphology for panels a−c. (B) FTIR imaging patterns showing the absorbance at 1456 cm^{-1}. This characteristic band allowed us to identify the conformational order, and panel a1 shows the optical micrograph for panel a. The sheared PLLA samples were submitted to crystallization at 135 °C for (a) 10, (b) 20, and (c) 30 min. The scale bars indicate 100 μm for all images.

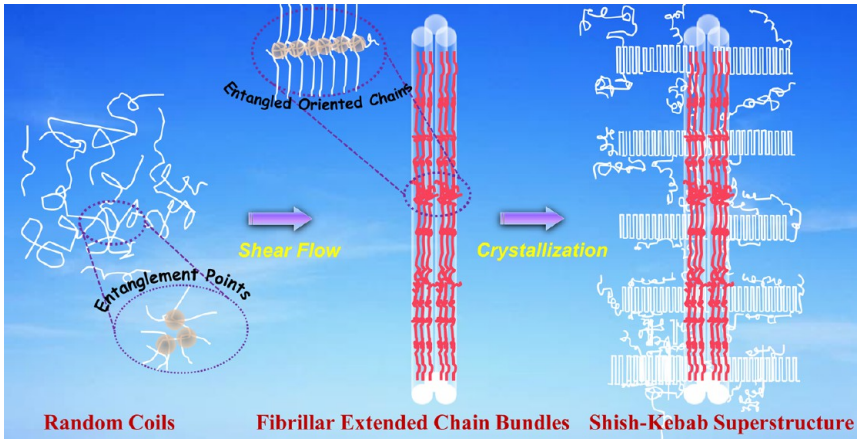

Figure 7. Schematic representation for the structural evolution of the shish-kebab superstructures in sheared PLLA. Of crucial importance are the existence of numerous chain ties bridging the extended, long and short chains that constitute the oriented shish. Once subjected to the pulse of shear, the oriented entangled chains form the fibrillar extended chain crystals (shish), providing nucleation sites for the lateral growth of lamellae perpendicular to the central shish. The shear flow direction is vertical.

scattering reflection of oriented crystalline entities is exclusively observed in sheared PLLA, displaying a pair of symmetrically sharp streaks in the equatorial direction and a pair of bulb-shape lobes in the meridional direction (Figure 5d−f). The two typical signals evidently reveal the generation of shear-aligned shish and oriented kebabs perpendicularly rooted at the shish, which share the same morphological features with our recently observed PLLA shish-kebabs during injection molding.[18] Nevertheless, no scattering reflection can be found in static PLLA, probably due to the random arrangement of lamellae with a large distribution of lamellar distance.[26] We notice that the long period (L) of sheared PLLA, reflecting a statistical averaging outcome for the lamellar spacing in shish and kebabs, presents a moderate decrease with the rise of crystallization temperature. Specifically, L climbs up from 25.8 nm for PLLA sheared at 130 °C to 27.1 and 30.3 nm for the samples sheared at 135 and 140 °C, respectively. The steady organization of the lamellar structures in the kebabs during the crystallization should be responsible for this, presuming that shish concentration only accounts for a relatively low ratio in shear-induced shish-kebabs. Essentially, the relatively compact and ordered alignment of chains in the kebabs at higher crystallization temperature may result in larger thickness for the lamellae, consequently yielding the higher lamellar spacing. This hypothesis is supported by the observation of a lower L at 22.8 nm for injection-molded PLLA containing shish-kebabs, resulting primarily from the poor crystallization kinetics under rapid cooling process.[18]

For recognition of structural evolution and identification of conformational changes that accompanied the growth of PLLA cylindrites, we employed the combination of direct POM observation and IR imaging, as shown in Figure 6. For the crystallization, Figure 6A illustrates the outer lamellae were allowed to grow steadily, while the size of central cores appeared to be almost unaltered. Figure 6B reveals that the conformational ordering of central cores was elicited, as

DOI: 10.1021/acssuschemeng.5b00320
ACS Sustainable Chem. Eng. 2015, 3, 1443−1452

evidenced by the gradually increased absorbance intensity at 1456 cm^{-1}.[59] Moreover, the conformational order of shear-induced shish was evidently higher than that of neighboring kebabs and self-nucleated spherulites. This probably lies in the fact that the shear-aligned chains are allowed to orderly pack their segments into the lamellae in an energy-saving, efficiently favorable manner.[26]

Overlapping the real space observations and the reciprocal space identifications allows us to unveil the first establishment of numerous shish-kebabs for PLLA in a transient shear flow, which may help to reveal fundamental understanding with respect to the origin and critical shear flow parameters of shish formation. At the same time this possesses great technological interest by enabling the manufacture of high-performance PLLA through time-saving processing without the compromise of properties caused by degradation of PLLA chains. Figure 7 schematically depicts the major structural features during the evolution of PLLA shish-kebabs. A short-term shear, although with high shear rate, is basically unable to fully stretch and orient chains, which can be further interfered by the immediate relaxation of oriented chain segments after the cessation of shear.[60] It encourages us to conceive that the chain entanglements of PLLA, naturally existing in the amorphous random coils and physically connecting neighboring chains, are of critical importance to assist the orientation of neighboring chains during the shear action and to stabilize the oriented chain segments through the network linkages after the cessation of shear. Thus, the stabilization and growth of oriented nucleation precursors are overwhelmingly preferred during the competition with simultaneous relaxation and recoil. This assumption is widely proposed in an assortment of polyolefin models, in which the presence of long chains is demonstrated to be vital to accommodate the concentration of chain entanglements and to trigger the shish formation.[41,61−63]

The investigations of the shish structures are central for disclosing the origin, mechanisms, and prerequisites of shish formation. Here the overgrowth of the shish permits unfolding its inner structure, displaying fibrillar extended chain crystals (Figures 3 and 7). This well supports the popular viewpoint that shish (primary row nuclei) is initiated from the shear-aligned bundles of parallel chain fragments that become thermodynamically stable.[64] The primary shish is generally characterized by a high degree of orientation but a low crystallinity (or in mesomorphic state), making it difficult to distinguish the inner structure by direct observations.[41] In our case, the crystallization procedure confers the adequate growth of shish along the flow direction, following the proposal of Petermann et al., at the same time providing nucleation sites for the lateral development of folded kebabs involving adjacent chains.[65] The scenario is favored because the bundles of extended chain crystals can also alleviate the local stress of the surrounding chains by encouraging the chain folding process through secondary nucleation.[60] Our observation of PLLA shish assembled by the bundles of fibrillar extended chain crystals again provides direct evidence for the traditional hypothesis of the shish structure.

In addition to the above complements on the theoretical cornerstones, our proposed methodology, i.e., the application of a pulse of intensive shear flow to trigger the formation of shish precursors, is instructive for fabricating high-performance PLLA products rich in shish-kebabs. Particularly, PLLA macromolecules are desirably protected from degradation given the short duration of strong shear and high temperature favoring higher resistance to external stress and impact, as well demonstrated in Figure 8. Unexpectedly, the weight-average

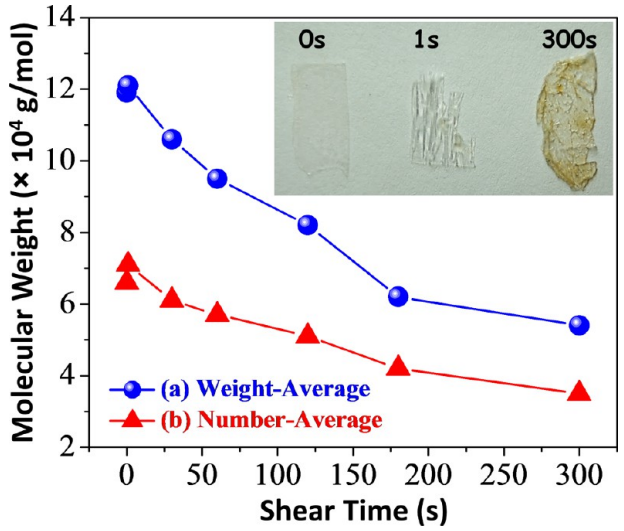

Figure 8. (a) Weight-average molecular weight (M_w) and (b) number-average molecular weight (M_n) of PLLA sheared at 135 °C as a function of shear time. The shear rate was held at 100 s^{-1}. The inset digital photo compares the appearance of PLLA samples after a shear of 0, 1, and 300 s (with an increased thickness of ~40 μm for direct comparison), implying that long duration of shear resulted in undesirable color changes caused by molecular degradation.

molecular weight (M_w) and number-average molecular weight (M_n) of PLLA subjected to a pulse of shear are at the comparable but slightly increased level (12.1×10^4 and 7.1×10^4, respectively), compared to those of the static samples (11.9×10^4 and 6.6×10^4, respectively). Employing longer duration of shear flow, however, leads to drastic fall in both M_w and M_n. In particular, it is worth mentioning that M_w of sheared PLLA is characterized by a sharper decline compared to M_n. For instance, PLLA sheared for 60 s presents a M_w of 9.5×10^4 and a M_n of 5.7×10^4 and the molecular weight further falls down to 6.2×10^4 and 4.2×10^4 after a shear of 180 s, respectively. It evidently suggests that long chains, suffering the large part of shear stress, are mainly involved in the random chain scissions in the shear, while the shorter chains are degraded to a smaller extent. The undesirable degradation of long chains during long shear times may cause unsatisfactory mechanical behaviors, assuming that the external impact and loading are first transferred through the long chains.[66]

More importantly, the shear-induced color degradation, as shown in the inset digital photo of Figure 8, may limit the commercial applications of PLLA subjected to long-lived shear. We anticipate that our time-saving approach will promote the concentration of shish-kebabs at the same time as shear-induced chain degradation is avoided. This will further advance the mechanical properties obtained after extrusion, blowing and injection molding of PLLA, in which the short-term and strong shear flow is normally generated, especially in the vicinity of the die. This approach could be broadly applicable to create highly oriented superstructures for various biopolymers and bioplastics, overcoming the challenges of high sensitivity to heat, poor crystallization kinetics and uncontrollable molecular arrangement, shaping the facile, rapid approach of fabricating bioplastics toward industrial-scale, low-cost, and high-performance commodities.

DOI: 10.1021/acssuschemeng.5b00320
ACS Sustainable Chem. Eng. 2015, 3, 1443−1452

CONCLUSIONS

The present work marks the first application of transient, intensive shear flow for shish-kebab formation in PLLA, contributing to the leap from practical polymer processing to theoretical model case establishment. Specifically, we utilized a pulse of shear flow featuring an extremely short duration of 1 s and a shear rate high to 100 s^{-1} to create shish precursors, which were further organized to oriented shish-kebabs through controlled isothermal crystallization at 130, 135, and 140 °C. By combining the real space observations of the inner structure of the shish-kebabs and the reciprocal space identifications of the structural features, we provide direct evidence that shish was essentially associated with the shear-aligned fibrillar chain bundles, following the traditional popular assumption established in polyolefins. The creation of fibrillar row cores in the pulse of shear supported the proposition that the chain entanglements, which may compellingly stretch and orient neighboring chains by physical bonding, were of vital importance to build oriented superstructures. By tracing the structural evolution during the crystallization, we found that the conformational ordering of shish was triggered in a more efficiently favorable manner, compared to that of kebabs and spherulites. More importantly, we demonstrate that the pulse of shear desirably preserved the high molecular weight of PLLA, while larger shear strain led to obvious color degradation derived from dramatic chain scissions, in particular for the longer chains responsible for the desired mechanical property enhancement. Our findings are instructive for the rational design of processing parameters during materials fabrication (e.g., spinning, blowing and extrusion) equally desirable for diverse applications of biopolyesters from aviation to packing. On the basis of this effort, further exploration of the critical shear flow parameters for the formation of PLLA shish-kebabs, e.g., shear temperature, shear rate and shear strain, will be carried out in our group.

ASSOCIATED CONTENT

Supporting Information

POM observation revealing the effects of sample thickness and shear gradient on the structural features of PLLA shish-kebabs, and Fourier transform infrared spectroscopy examining the possibility of oxidization. The Supporting Information is available free of charge on the ACS Publications website at DOI: 10.1021/acssuschemeng.5b00320.

AUTHOR INFORMATION

Corresponding Authors

*L. Xie. E-mail: l.xie@sheffield.ac.uk.
*M. Hakkarainen. E-mail: minna@kth.se.

Notes

The authors declare no competing financial interest.

ACKNOWLEDGMENTS

The authors are deeply indebted to Dr. Patrick Baker from the Department of Molecular Biology and Biotechnology, University of Sheffield for his kind help during the X-ray measurements. H.X. and L.X. are grateful to the financial support from the China Scholarship Council (CSC) for studying abroad.

REFERENCES

(1) Keum, J. K.; Zuo, F.; Hsiao, B. S. Formation and stability of shear-induced shish-kebab structure in highly entangled melts of UHMWPE/HDPE blends. *Macromolecules* **2008**, *41*, 4766−4776.
(2) Somani, R. H.; Yang, L.; Zhu, L.; Hsiao, B. S. Flow-induced shish-kebab precursor structures in entangled polymer melts. *Polymer* **2005**, *46*, 8587−8623.
(3) Hsiao, B. S.; Yang, L.; Somani, R. H.; Avila-Orta, C. A.; Zhu, L. Unexpected shish-kebab structure in a sheared polyethylene melt. *Phys. Rev. Lett.* **2005**, *94*, 117802.
(4) Zhang, L.; Shi, W.; Cheng, H.; Han, C. C. Reexamination of shish kebab formation in poly(ethylene oxide) melts. *Polymer* **2014**, *55*, 2890−2899.
(5) Kimata, S.; Sakurai, T.; Nozue, Y.; Kasahara, T.; Yamaguchi, N.; Karino, T.; Shibayama, M.; Kornfield, J. A. Molecular basis of the shish-kebab morphology in polymer crystallization. *Science* **2007**, *316*, 1014−1017.
(6) Xu, H.; Xie, L.; Jiang, X.; Hakkarainen, M.; Chen, J.-B.; Zhong, G.-J.; Li, Z.-M. Structural basis for unique hierarchical cylindrites induced by ultrahigh shear gradient in single natural fiber reinforced poly(lactic acid) green composites. *Biomacromolecules* **2014**, *15*, 1676−1686.
(7) Shinohara, Y.; Yamazoe, K.; Sakurai, T.; Kimata, S.; Maruyama, T.; Amemiya, Y. Effect of structural inhomogeneity on mechanical behavior of injection molded polypropylene investigated with microbeam X-ray scattering. *Macromolecules* **2012**, *45*, 1398−1407.
(8) Schroer, C.; Kuhlmann, M.; Roth, S.; Gehrke, R.; Stribeck, N.; Almendarez-Camarillo, A.; Lengeler, B. Mapping the local nanostructure inside a specimen by tomographic small-angle X-ray scattering. *Appl. Phys. Lett.* **2006**, *88*, 164102.
(9) Zhao, Y.; Hayasaka, K.; Matsuba, G.; Ito, H. In situ observations of flow-induced precursors during shear flow. *Macromolecules* **2012**, *46*, 172−178.
(10) Kalay, G.; Kalay, C. R. Interlocking shish-kebab morphology in polybutene-1. *J. Polym. Sci., Polym. Phys.* **2002**, *40*, 1828−1834.
(11) Zhao, P.; Wang, K.; Yang, H.; Zhang, Q.; Du, R.; Fu, Q. Excellent tensile ductility in highly oriented injection-molded bars of polypropylene/carbon nanotubes composites. *Polymer* **2007**, *48*, 5688−5695.
(12) Wang, K.; Chen, F.; Zhang, Q.; Fu, Q. Shish−kebab of polyolefin by "melt manipulation" strategy in injection-molding: A convenience pathway from fundament to application. *Polymer* **2008**, *49*, 4745−4755.
(13) Yang, J.; Wang, C.; Wang, K.; Zhang, Q.; Chen, F.; Du, R.; Fu, Q. Direct formation of nanohybrid shish-kebab in the injection molded bar of polyethylene/multiwalled carbon nanotubes composite. *Macromolecules* **2009**, *42*, 7016−7023.
(14) Somani, R. H.; Hsiao, B. S.; Nogales, A. Structure development during shear flow induced crystallization of i-PP: In situ wide-angle X-ray diffraction study. *Macromolecules* **2001**, *34*, 5902−5909.
(15) Murase, H.; Ohta, Y.; Hashimoto, T. A new scenario of shish-kebab formation from homogeneous solutions of entangled polymers: Visualization of structure evolution along the fiber spinning line. *Macromolecules* **2011**, *44*, 7335−7350.
(16) Matsuba, G.; Sakamoto, S.; Ogino, Y.; Nishida, K.; Kanaya, T. Crystallization of polyethylene blends under shear flow. Effects of crystallization temperature and ultrahigh molecular weight component. *Macromolecules* **2007**, *40*, 7270−7275.
(17) Zhong, Y.; Fang, H.; Zhang, Y.; Wang, Z.; Yang, J.; Wang, Z. Rheologically determined critical shear rates for shear-induced nucleation rate enhancements of poly(lactic acid). *ACS Sustainable Chem. Eng.* **2013**, *1*, 663−672.
(18) Xu, H.; Zhong, G.-J.; Fu, Q.; Lei, J.; Jiang, W.; Hsiao, B. S.; Li, Z.-M. Formation of shish-kebabs in injection-molded poly(L-lactic acid) by application of an intense flow field. *ACS Appl. Mater. Interfaces* **2012**, *4*, 6774−6784.
(19) Fang, H.; Zhang, Y.; Bai, J.; Wang, Z. Shear-induced nucleation and morphological evolution for bimodal long chain branched polylactide. *Macromolecules* **2013**, *46*, 6555−6565.

DOI: 10.1021/acssuschemeng.5b00320
ACS Sustainable Chem. Eng. 2015, 3, 1443−1452

(20) Xu, H.; Xie, L.; Chen, J.-B.; Jiang, X.; Hsiao, B. S.; Zhong, G.-J.; Fu, Q.; Li, Z.-M. Strong and tough micro/nanostructured poly(lactic acid) by mimicking multifunctional hierarchy of shell. *Mater. Horiz.* **2014**, *1*, 546−552.
(21) Kalb, B.; Pennings, A. General crystallization behaviour of poly(L-lactic acid). *Polymer* **1980**, *21*, 607−612.
(22) Tang, H.; Chen, J.-B.; Wang, Y.; Xu, J.-Z.; Hsiao, B. S.; Zhong, G.-J.; Li, Z.-M. Shear flow and carbon nanotubes synergistically induced nonisothermal crystallization of poly(lactic acid) and its application in injection molding. *Biomacromolecules* **2012**, *13*, 3858−3867.
(23) Diop, M. F.; Burghardt, W. R.; Torkelson, J. M. Well-mixed blends of HDPE and ultrahigh molecular weight polyethylene with major improvements in impact strength achieved via solid-state shear pulverization. *Polymer* **2014**, *55*, 4948−4958.
(24) Plackett, D.; Løgstrup Andersen, T.; Batsberg Pedersen, W.; Nielsen, L. Biodegradable composites based on L-polylactide and jute fibres. *Compos. Sci. Technol.* **2003**, *63*, 1287−1296.
(25) Liang, S.; Wang, K.; Yang, H.; Zhang, Q.; Du, R.; Fu, Q. Crystal morphology and tensile properties of LLDPE containing PP fibers as obtained via dynamic packing injection molding. *Polymer* **2006**, *47*, 7115−7122.
(26) Xu, H.; Xie, L.; Chen, Y.-H.; Huang, H.-D.; Xu, J.-Z.; Zhong, G.-J.; Hsiao, B. S.; Li, Z.-M. Strong shear flow-driven simultaneous formation of classic shish-kebab, hybrid shish-kebab, and trans-crystallinity in poly(lactic acid)/natural fiber biocomposites. *ACS Sustainable Chem. Eng.* **2013**, *1*, 1619−1629.
(27) Ojijo, V.; Ray, S. S.; Sadiku, R. Toughening of biodegradable polylactide/poly (butylene succinate-co-adipate) blends via in situ reactive compatibilization. *ACS Appl. Mater. Interfaces* **2013**, *5*, 4266−4276.
(28) Xie, L.; Xu, H.; Wang, Z.-P.; Li, X.-J.; Chen, J.-B.; Zhang, Z.-J.; Yin, H.-M.; Zhong, G.-J.; Lei, J.; Li, Z.-M. Toward faster degradation for natural fiber reinforced poly(lactic acid) biocomposites by enhancing the hydrolysis-induced surface erosion. *J. Polym. Res.* **2014**, *21*, 357−371.
(29) Andersson, S. R.; Hakkarainen, M.; Inkinen, S.; Södergård, A.; Albertsson, A.-C. Customizing the hydrolytic degradation rate of stereocomplex PLA through different PDLA architectures. *Biomacromolecules* **2012**, *13*, 1212−1222.
(30) Inkinen, S.; Hakkarainen, M.; Albertsson, A.-C.; Södergård, A. From lactic acid to poly(lactic acid) (PLA): Characterization and analysis of PLA and its precursors. *Biomacromolecules* **2011**, *12*, 523−532.
(31) Xu, H.; Liu, C.-Y.; Chen, C.; Hsiao, B. S.; Zhong, G.-J.; Li, Z.-M. Easy alignment and effective nucleation activity of ramie fibers in injection-molded poly(lactic acid) biocomposites. *Biopolymers* **2012**, *97*, 825−839.
(32) Martínez-Sanz, M.; Lopez-Rubio, A.; Lagaron, J. M. Optimization of the dispersion of unmodified bacterial cellulose nanowhiskers into polylactide via melt compounding to significantly enhance barrier and mechanical properties. *Biomacromolecules* **2012**, *13*, 3887−3899.
(33) Xie, L.; Xu, H.; Niu, B.; Ji, X.; Chen, J.; Li, Z.-M.; Hsiao, B. S.; Zhong, G.-J. Unprecedented access to strong and ductile poly(lactic acid) by introducing in situ nanofibrillar poly(butylene succinate) for green packaging. *Biomacromolecules* **2014**, *15*, 4054−4064.
(34) Carosio, F.; Colonna, S.; Fina, A.; Rydzek, G.; Hemmerlé, J.; Jierry, L.; Schaaf, P.; Boulmedais, F. Efficient gas and water vapor barrier properties of thin poly(lactic acid) packaging films: Functionalization with moisture resistant nafion and clay multilayers. *Chem. Mater.* **2014**, *26*, 5459−5466.
(35) Aulin, C.; Karabulut, E.; Tran, A.; Wågberg, L.; Lindström, T. Transparent nanocellulosic multilayer thin films on polylactic acid with tunable gas barrier properties. *ACS Appl. Mater. Interfaces* **2013**, *5*, 7352−7359.
(36) Xu, H.; Wu, D.; Yang, X.; Xie, L.; Hakkarainen, M. Thermostable and impermeable "nano-barrier walls" constructed by poly(lactic acid) stereocomplex crystal decorated graphene oxide nanosheets. *Macromolecules* **2015**, *48*, 2127−2137.
(37) Pennings, A. J.; Kiel, A. M. Fractionation of polymers by crystallization from solution, III. On the morphology of fibrillar polyethylene crystals grown in solution. *Kolloid Z. Z. Polym.* **1965**, *205*, 160−162.
(38) Binsbergen, F. L. Orientation-induced nucleation in polymer crystallization. *Nature* **1966**, *211*, 516−517.
(39) Hayashi, Y.; Matsuba, G.; Zhao, Y.; Nishida, K.; Kanaya, T. Precursor of shish−kebab in isotactic polystyrene under shear flow. *Polymer* **2009**, *50*, 2095−2103.
(40) Cavallo, D.; Azzurri, F.; Balzano, L.; Funari, S. r. S.; Alfonso, G. C. Flow memory and stability of shear-induced nucleation precursors in isotactic polypropylene. *Macromolecules* **2010**, *43*, 9394−9400.
(41) Balzano, L.; Rastogi, S.; Peters, G. Self-nucleation of polymers with flow: The case of bimodal polyethylene. *Macromolecules* **2011**, *44*, 2926−2933.
(42) Balzano, L.; Rastogi, S.; Peters, G. W. M. Crystallization and precursors during fast short-term shear. *Macromolecules* **2009**, *42*, 2088−2092.
(43) Yan, T.; Zhao, B.; Cong, Y.; Fang, Y.; Cheng, S.; Li, L.; Pan, G.; Wang, Z.; Li, X.; Bian, F. Critical strain for shish-kebab formation. *Macromolecules* **2010**, *43*, 602−605.
(44) Mykhaylyk, O. O.; Chambon, P.; Graham, R. S.; Fairclough, J. P. A.; Olmsted, P. D.; Ryan, A. J. The specific work of flow as a criterion for orientation in polymer crystallization. *Macromolecules* **2008**, *41*, 1901−1904.
(45) Mykhaylyk, O. O.; Chambon, P.; Impradice, C.; Fairclough, J. P. A.; Terrill, N. J.; Ryan, A. J. Control of structural morphology in shear-induced crystallization of polymers. *Macromolecules* **2010**, *43*, 2389−2405.
(46) Housmans, J.-W.; Steenbakkers, R. J. A.; Roozemond, P. C.; Peters, G. W. M.; Meijer, H. E. H. Saturation of pointlike nuclei and the transition to oriented structures in flow-induced crystallization of isotactic polypropylene. *Macromolecules* **2009**, *42*, 5728−5740.
(47) D'Haese, M.; Mykhaylyk, O. O.; Van Puyvelde, P. On the onset of oriented structures in flow-induced crystallization of polymers: A comparison of experimental techniques. *Macromolecules* **2011**, *44*, 1783−1787.
(48) Cong, Y.; Liu, H.; Wang, D.; Zhao, B.; Yan, T.; Li, L.; Chen, W.; Zhong, Z.; Lin, M.-C.; Chen, H.-L.; Yang, C. Stretch-induced crystallization through single molecular force generating mechanism. *Macromolecules* **2011**, *44*, 5878−5882.
(49) Zhang, C.; Hu, H.; Wang, D.; Yan, S.; Han, C. C. In situ optical microscope study of the shear-induced crystallization of isotactic polypropylene. *Polymer* **2005**, *46*, 8157−8161.
(50) Zhang, C.; Hu, H.; Wang, X.; Yao, Y.; Dong, X.; Wang, D.; Wang, Z.; Han, C. C. Formation of cylindrite structures in shear-induced crystallization of isotactic polypropylene at low shear rate. *Polymer* **2007**, *48*, 1105−1115.
(51) Wang, Y.; Meng, K.; Hong, S.; Xie, X.; Zhang, C.; Han, C. C. Shear-induced crystallization in a blend of isotactic polypropylene and high density polyethylene. *Polymer* **2009**, *50*, 636−644.
(52) Li, X.-J.; Zhong, G.-J.; Li, Z.-M. Non-isothermal crystallization of poly(L-lactide) (PLLA) under quiescent and steady shear conditions. *Chin. J. Polym. Sci.* **2010**, *28*, 357−366.
(53) Yamazaki, S.; Itoh, M.; Oka, T.; Kimura, K. Formation and morphology of "shish-like" fibril crystals of aliphatic polyesters from the sheared melt. *Eur. Polym. J.* **2010**, *46*, 58−68.
(54) Huang, S.; Li, H.; Jiang, S.; Chen, X.; An, L. Crystal structure and morphology influenced by shear effect of poly(L-lactide) and its melting behavior revealed by WAXD, DSC and in-situ POM. *Polymer* **2011**, *52*, 3478−3487.
(55) Somani, R. H.; Hsiao, B. S.; Nogales, A.; Srinivas, S.; Tsou, A. H.; Sics, I.; Balta-Calleja, F. J.; Ezquerra, T. A. Structure development during shear flow-induced crystallization of iPP: In-situ small-angle X-ray scattering study. *Macromolecules* **2000**, *33*, 9385−9394.

DOI: 10.1021/acssuschemeng.5b00320
ACS Sustainable Chem. Eng. 2015, 3, 1443−1452

(56) Yang, L.; Somani, R. H.; Sics, I.; Hsiao, B. S.; Kolb, R.; Fruitwala, H.; Ong, C. Shear-induced crystallization precursor studies in model polyethylene. *Macromolecules* **2004**, *37*, 4845−4859.
(57) Dikovsky, D.; Marom, G.; Avila-Orta, C. A.; Somani, R. H.; Hsiao, B. S. Shear-induced crystallization in isotactic polypropylene containing ultra-high molecular weight polyethylene oriented precursor domains. *Polymer* **2005**, *46*, 3096−3104.
(58) Xu, H.; Xie, L.; Jiang, X.; Li, X.-J.; Li, Y.; Zhang, Z.-J.; Zhong, G.-J.; Li, Z.-M. Toward stronger transcrystalline layers in poly(L-lactic acid)/natural fiber biocomposites with the aid of an accelerator of chain mobility. *J. Phys. Chem. B* **2014**, *118*, 812−823.
(59) Zhang, J.; Tsuji, H.; Noda, I.; Ozaki, Y. Structural changes and crystallization dynamics of poly(L-lactide) during the cold-crystallization process investigated by infrared and two-dimensional infrared correlation spectroscopy. *Macromolecules* **2004**, *37*, 6433−6439.
(60) Somani, R. H.; Yang, L.; Hsiao, B. S.; Agarwal, P. K.; Fruitwala, H. A.; Tsou, A. H. Shear-induced precursor structures in isotactic polypropylene melt by in-situ rheo-SAXS and rheo-WAXD studies. *Macromolecules* **2002**, *35*, 9096−9104.
(61) Zhao, B.; Li, X.; Huang, Y.; Cong, Y.; Ma, Z.; Shao, C.; An, H.; Yan, T.; Li, L. Inducing crystallization of polymer through stretched network. *Macromolecules* **2009**, *42*, 1428−1432.
(62) Azzurri, F.; Alfonso, G. C. Insights into formation and relaxation of shear-induced nucleation precursors of isotactic PS. *Macromolecules* **2008**, *41*, 1377−1383.
(63) Hashimoto, T.; Murase, H.; Ohta, Y. A new scenario of flow-induced shish-kebab formation in entangled polymer solutions. *Macromolecules* **2010**, *43*, 6542−6548.
(64) Somani, R. H.; Yang, L.; Hsiao, B. S. Effects of high molecular weight species on shear-induced orientation and crystallization of isotactic polypropylene. *Polymer* **2006**, *47*, 5657−5668.
(65) Lieberwirth, I.; Loos, J.; Petermann, J.; Keller, A. Observation of shish crystal growth into nondeformed melts. *J. Polym. Sci., Polym. Phys.* **2000**, *38*, 1183−1187.
(66) Jud, K.; Kausch, H. Load transfer through chain molecules after interpenetration at interfaces. *Polym. Bull.* **1979**, *1*, 697−707.

DOI: 10.1021/acssuschemeng.5b00320
ACS Sustainable Chem. Eng. 2015, 3, 1443−1452